Liu, Y., Sun, P., Niu, H., Huang, X., & Rein, G. (2021). Propensity to self-heating ignition of open-circuit pouch lithium-ion battery pile on a hot boundary. Fire Safety Journal, 120, 103081. https://doi.org/10.1016/j.firesaf.2020.103081

Propensity to self-heating ignition of open-circuit pouch Lithium-ion battery pile on a hot boundary

Yanhui Liu[a,b], Peiyi Sun[a], Huichang Niu[b], Xinyan Huang[a,*], Guillermo Rein[c]

[a]*Research Centre for Fire Engineering, The Hong Kong Polytechnic University, Hong Kong*

[b]*Institute of Industry Technology, Guangzhou & Chinese Academy of Sciences, China*

[c]*Department of Mechanical Engineering, Imperial College London, UK*

Highlights:

- Study self-ignition of open-circuit pouch Li-ion battery via the classical hot-plate test
- Critical boundary temperature for thermal runaway increases with battery pile thickness
- Insulated boundary reduces the self-ignition temperature of the battery pile by 20 K

Abstract:

The fire safety issue of Lithium-ion (Li-ion) batteries is an important obstacle for its market growth and applications. Although the open-circuit condition (e.g. storage, transport and disposal) accounts for the major part of battery lifespan, little research has investigated its self-ignition hazard during non-operating periods. In this work, we experimentally study the self-heating behavior of piled pouch Li-ion battery cells through the classical hot-plate experiments. Results show that the self-ignition of battery occurs under a hot plate temperature ranging from 199 °C to 262 °C, depending on the number of cells and environmental cooling. Thermal runaway always first occurs to the cell next to the hot plate and then propagates to upper cells. This critical temperature is increased by 20 °C under a good environmental cooling condition whereas it is reduced by 40 °C as the state of charge increases from 30% to 80%. Moreover, the critical plate temperature for self-ignition increases slightly with the height of battery pile, which is opposite to both hot-plate experiments of hydrocarbon materials and the oven experiments of battery. Therefore, the classical self-ignition theory may not be applicable for Li-ion batteries next to a hot boundary. This research reveals new self-ignition phenomena and helps understand the fire safety of Li-ion batteries in storage and transport.

Keywords: battery fire; thermal runaway; self-ignition; size effect

1. Introduction

Due to the high energy density and outstanding working performance, Lithium-ion (Li-ion) batteries (LIB) are widely used in most of the portable electric devices and energy-storage systems [1,2]. However, their fire safety is still a major concern due to the lower thermal stability [3]. Over the last 30 years, numerous fire accidents of Li-ion batteries have been reported, indicating that the current battery system is far from fire-safe [4,5]. For example, in 2016, many LIBs of Galaxy Note 7 smartphones 'self-ignited' during the use, which was eventually banned by many airlines and resulted in an economic loss of more than $10 billion [6] (Fig. 1a). Also, there have been several serious fire accidents in electric vehicle such as the Tesla Model S [7–9] (Fig. 1b), and some fires were 'self-ignited' during driving (discharging) or charging. The active, volatile and flammable materials like Li element and electrolyte compound [10] used in Li-ion batteries have posed a serious threat to numerous energy-storage devices and billions of end-users worldwide [11].

In general, the Li-ion batteries are more vulnerable when they subject to the thermal, electrical, and mechanical impacts [12,13]. These impacts could trigger strong thermochemical and electrochemical reactions inside batteries, generating a large amount of toxic and combustible gases. Eventually, the thermal runaway of the Li-ion battery can lead to the burning of flammable smoke [14] and gas jet [15,16] or even explosion [17]. Abaza *et al*. [18] studied the thermal runaway behavior of commercial pouch batteries under internal and external short circuit cases and revealed the conductivity of nail materials influences the shorting resistance and the thermal runaway behavior. Zhu *et al*. [19] investigated the overcharge-induced thermal runaway features of pouch Li-ion batteries under different current rates and concluded the higher current rate is easier to cause the thermal runaway because of the dramatic side reactions. Gao *et al*. [20] recently showed that the voltage waving can be utilized to determine the thermal runaway propagation time and the pouch battery module in parallel has poor safety than module in series.

Figure 1 (a) A smartphone caught fire as a result of battery self-ignition, (b) A Tesla Model S caught fire due to traffic accident in 2013, (c) An aviation container carrying Li-ion batteries caught fire at Hong Kong International Airport in 2019, and (d) fire of Li-ion battery warehouse in China in 2014.

Most of the past studies focused on battery fires initiated or 'self-ignited' under extreme operating conditions such as external heating, short circuit, fast-charging, and over-discharging (e.g. during the fast acceleration of EV). Note that these so-called 'self-ignition' phenomena are still heated internally by the Joule heat and operation current, which is fundamentally different from classical self-ignition phenomena of solid fossil fuels like coals and biomass silos [21]. Nevertheless, little research has studied the self-ignition risk of non-operating (or open-circuit without operation current) Li-ion battery piles, although the open-circuit condition accounts for the major part of battery lifespan. In recent years, many catastrophic fires happened to open-circuit Li-ion batteries worldwide. For example, in 2010, a Boeing 744 operated by UPS Airlines crashed in Dubai because of an in-flight fire due to the self-ignition of 81,000 Li-ion batteries in cargo. Similarly, in 2019, an aviation container in the Hong Kong International Airport carrying Li-ion batteries burst into flames and released a large amount of smoke [22] (Fig. 1c). Moreover, there have also been many fire accidents in open-circuit batteries in the warehouse (Fig. 1d).

The self-heating ignition occurs when the heat release rate from exothermic chemical reactions exceeds the environmental cooling rate [21]. Because of the exothermic reactions involving the electrodes and electrolyte, the Li-ion battery can undergo self-heating in the absence of external impact. By increasing the internal temperature, it creates a localized failure inside the battery and promotes other exothermic reactions that eventually lead to thermal runaway. Even if the self-heating does not lead to a fire, it still can increase the possibility of future battery fire accidents. The size is another important safety concern for self-ignition. In practice, larger batteries and battery system are preferred for storage, transportation and application, but a larger size can have a higher risk of self-ignition. Recently, He *et al.* [23] found that for the self-ignition of prismatic Li-ion battery cells (up to 4 cells), the critical ambient temperature decreases as the number of cells increase, showing a similar trend to other organic solid fuels. Therefore, it is urgent to understand more about the self-ignition risk of Li-ion batteries and develop safety principles for the large scale of battery.

This paper investigates the self-heating ignition behavior of pouch Li-ion battery cells under a hot boundary condition through a classical hot-plate self-ignition test apparatus. The minimum boundary temperature to trigger the thermal runaway of battery is quantified under different cell-layer number and the environmental cooling conditions. A simplified 1-D heat-transfer analysis is used to explain the trend of thermal-runaway criteria of Li-ion battery and compare with conventional hydrocarbon fuels.

2. Experimental setup

2.1. Battery samples

There are three types of Li-ion battery cells: cylindrical, prismatic and pouch [24]. The pouch battery is becoming more popular due to the advantages of large energy capacity, lightweight, and flexible shape design, so it has been widely used in mobile phones, tablet computers, electronic cigarettes and electric vehicles. Nevertheless, compared with cylindrical cells, once the thermal runaway occurred, pouch cells may produce a higher temperature and pressure due to a higher energy density and the lack of safety vent [13].

In this experiment, a small pouch cell, made in Shenzhen, China, was tested. This battery has been widely used in small electric devices such as digital camera, drone, and sweeping robot. As shown in Fig. 2(a), the pouch cell is essentially a flat layer with the dimension of 40 mm (length) × 30 mm (width) × 10 mm (thickness) and an original mass of 21.40 ± 0.05 g, which is similar to the prismatic cell (50 mm × 34 mm × 10 mm) used in the past hot-oven test [23].

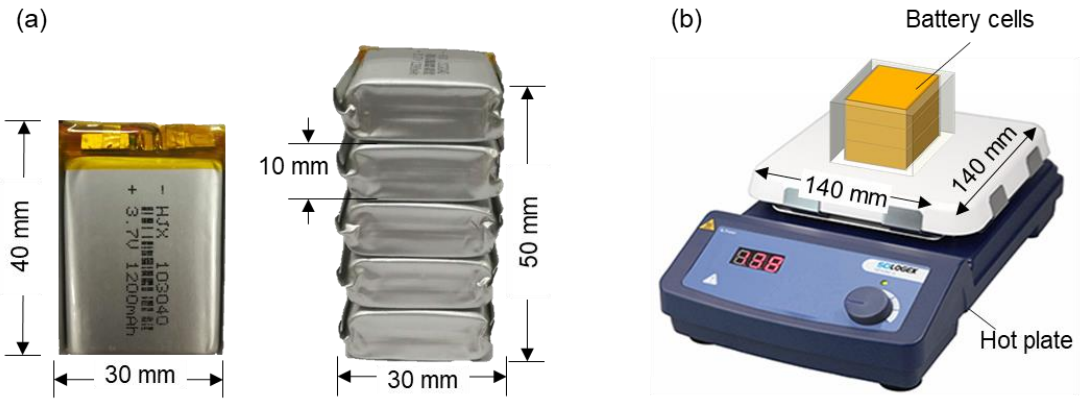

Figure 2 (a) Photo of pouch battery and battery stack, and (b) diagram of the hot-plate experimental setup.

The positive electrode material of this pouch cell uses the Lithium Nickel Manganese Cobalt Oxide ($LiNi_xMn_yCo_zO_2$ or NMC). The state of charge for each battery was calibrated before the test. Each battery cell was fully charged with constant-voltage mode to 100% state of charge (SOC) and then discharged with a constant current of 600 mA until the SOC of 80% or 30%. After the charging and discharging process, the battery rested for at least 3 hours to avoid the influence of internal heating during the preparation. The physical parameters and charge-discharge characteristics of the pouch cell are shown in Table 1.

Table 1. Physical and charge-discharge parameters of the pouch Li-ion battery cell.

Dimension (mm)	Mass (g)	Nominal capacity (Ah)	Nominal voltage (V)	Charging cut-off voltage (V)	Discharging cut-off voltage (V)
40×30×10	21.35	1.2	3.7	4.15 ± 0.05	3.05 ± 0.05

2.2. Test setup

To better characterize the self-heating ignition process of battery cells, the experimental setup adopted the standard test method for hot surface self-ignition of dust layers, i.e., the ASTME 2021 test or the standard hot-plate test [25]. A Thermofisher HP88850105 hot plate with the temperature accuracy of ±1 ℃ was used to provide a hot boundary of the constant temperature up to 550 ℃. Above the hot plate, there was a vertical stack of open-circuit pouch cells, i.e., open circuit, as shown in Fig. 2b. Four sides of the battery pile were surrounded by 10-mm ceramic insulation boards with the thermal conductivity of $0.12\ \mathrm{W/m \cdot K}$ and the thermal resistance of $0.083\mathrm{m}^2\ \mathrm{K/W}$. The temperature distribution of the battery cells was monitored by several thin K-type thermocouples with the bead diameter of 0.2 mm and the accuracy of 0.1 ℃. The thermocouples were placed in the round corner of the battery, so they would not affect the contact between battery cells (Fig. 3).

The data logger was used to collect the temperature information and the voltage of each battery cell. Before and after the experiment, the mass for each battery cell was measured by a scale (±0.01 g). A video camera was used to record the front view of the entire experiment process.

2.3. Controlling parameters and procedures

In this study, all tests are conducted under ambient temperature (T_a) of 25 ± 2°C and the relative humidity of 50-70%. Three key test parameters are controlled:

(1) *Number of layers or cells (N)*. The layer of the battery pile ranges from 1 to 5, and the height for each layer is 10 mm, that is, the height of the battery pile ranges from 10 to 50 mm, as shown in Figs. 2 and 3.

(2) *State of Charge (SOC)*. Two SOCs of 30% and 80% are chosen, as most of the Li-ion batteries are operated in between these values. In general, the higher SOC means the larger fire risk [12,13], so that SOC of 80% is examined in more detail.

(3) *Top boundary cooling condition*. Three different cooling conditions on the battery top surface are tested, as illustrated in Fig. 3:

- Good cooling. The top surface is exposed to air directly, that is, the height of the surrounding insulation boards is equal to the height of the battery pile (Fig. 3a);
- Weak cooling. The surrounding insulation board is higher than the battery pile, which is fixed to 50 mm to limit the free convective cooling (Fig. 3b);
- Insulated. The battery top boundary is covered by the insulation board to minimize environmental cooling (Fig. 3c).

The hot plate is first preheated to the target boundary temperature (T_b), ranging from 150 °C to 300 °C. Once the targeted temperature is reached, it is stabilized for at least 10 min. Then, the prepared battery pile is carefully placed in the center of hot-plate, ensuring good contact between the bottom surface of the battery pile and the top surface of the hot-plate. The actual temperature of the hot boundary is monitored by thin thermocouples that are fixed on several different locations of the hot plate (see Fig. 3), which has an uncertainty of within ±1 °C based on repeating tests.

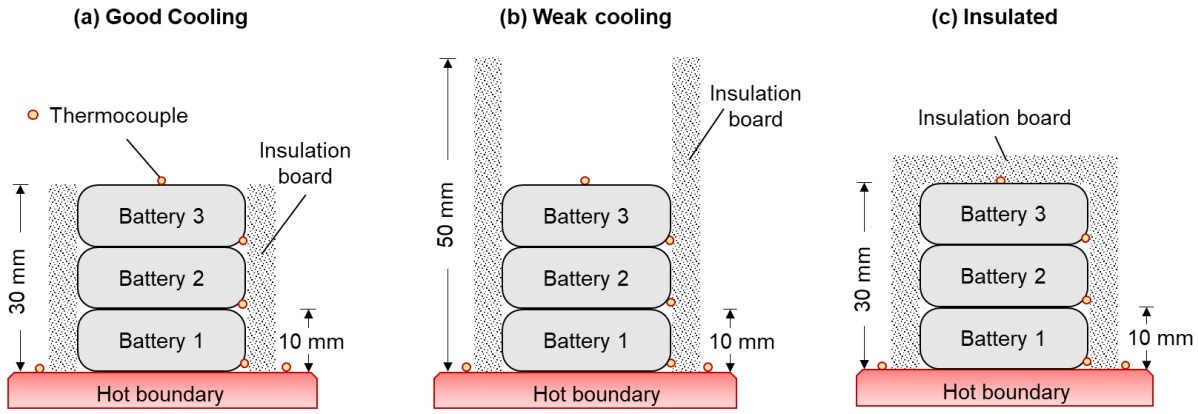

Figure 3. The schematic of three top boundary condition (a) good cooling, (b) weak cooling, and (c) insulated where three layers of pouch Li-ion batteries are used for illustration and locations of thermocouples are marked.

The *supercritical ignition temperature* is defined as the minimum hot boundary temperature that allows the thermal runaway to happen, and the *subcritical temperature* is defined as the maximum hot boundary temperature that prevents the thermal runaway. Experiments were conducted under different hot-boundary temperatures until the temperature difference between the supercritical and subcritical ignition temperature was within 5 °C. Then, the critical boundary temperature for the self-heating ignition is the average value of supercritical and subcritical temperatures. To ensure the experimental repeatability, at least two repeating tests were conducted, and especially more tests were repeated near the critical conditions.

3. Experimental results

Referring to the standard test method for the hot surface self-ignition test ASTME 2021 [26], two criteria could be used to determine whether the thermal runaway of tested pouch battery occurs or not:

i. The temperature of battery surface is higher than the temperature of hot boundary for at least 50 °C and rise sharply; or

ii. The battery releases a large amount of smoke, and the surface becomes black in accompany with a clear electrolyte leakage.

If either criterion is satisfied, the battery is considered going through thermal runaway.

3.1. Thermal runaway phenomena

Figure 4 shows the typical experimental processes of a successful and a failed thermal runaway with the five-layer battery pile under a good environmental cooling. For the successful thermal runaway in Fig. 4a, the bottom boundary temperature was constant at 230 °C. During the heating, batteries first started to swell at 370 s, which indicates the initiation of internal chemical reactions and gas generation. During the swelling process, a small amount of gas was leaked from the bottom cell, because the pouch cell cannot withstand high internal pressure. From the video, the cell continued to swell until about 12 mm, i.e., about a 20% increase in thickness. At 2260 s, it suddenly released a large amount of smoke, i.e., the thermal runaway.

In all tested cases of thermal runaway, the bottom cell next to the hot plate reached the thermal runaway first, so that it is the most dangerous cell. Then, the thermal runaway would start to propagate upward cell by cell with a time interval of about 20 s until all cells went thermal runaway. Note that unlike the common cylindrical battery with a safety vent [16], the thermal runaway of this pouch battery occurred without a visible flame. It is mainly because there is neither a safety vent to produce a fast gas jet nor a metal shell to allow the friction with the jet flow to generate sparks. Nevertheless, with a pilot flame near the smoke, a flame was easily initiated and sustain the burning of battery.

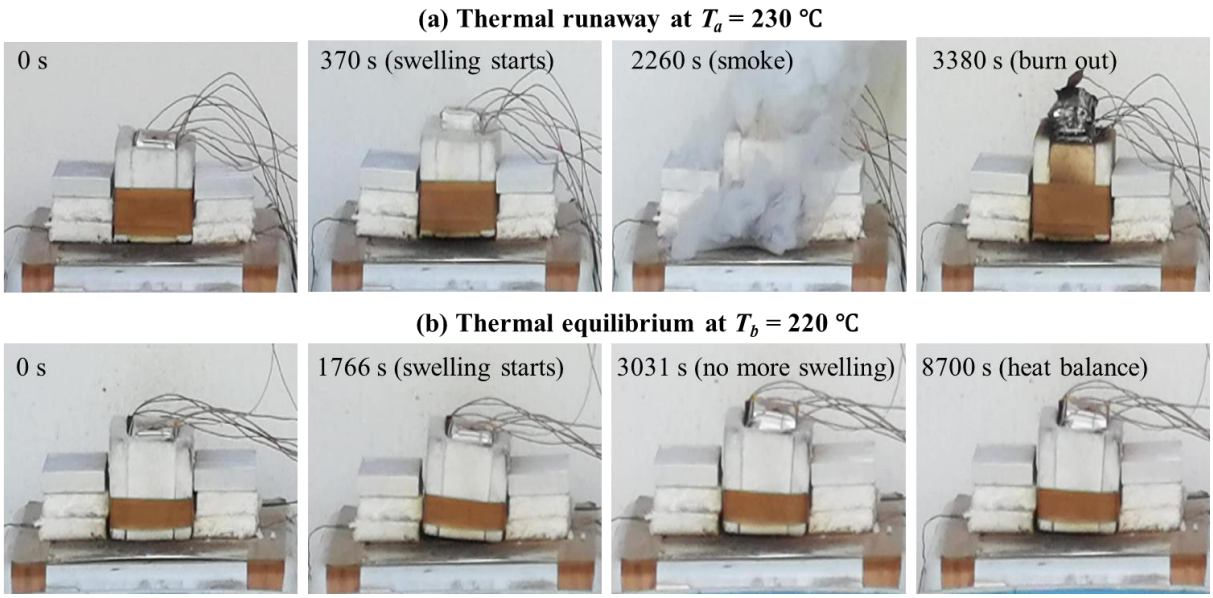

Figure 4. Phenomena of a 5-layer battery pile of 80% SOC under a good top cooling condition: (a) thermal runaway occurs at the hot plate of 230℃, and (b) thermal equilibrium is reached at the hot plate of 220℃.

For the case of failed thermal runaway in Fig. 4b, the bottom boundary temperature was constant at 220 °C. During the heating process, there was no clear release of the smoke, so that it was not clear whether the electrolyte leaked or not. At the same time, the swelling process continued until about 3031 s, and the final degree of swelling was about 20%, similar to the case of thermal runaway. Afterwards, all battery cells reached the heat balance, and no thermal runaway was observed even after another ten hours on the hot plate. Further reducing the temperature gap, the critical hot boundary temperature for thermal runaway (T_b^*) was found to be 223 ± 2 °C.

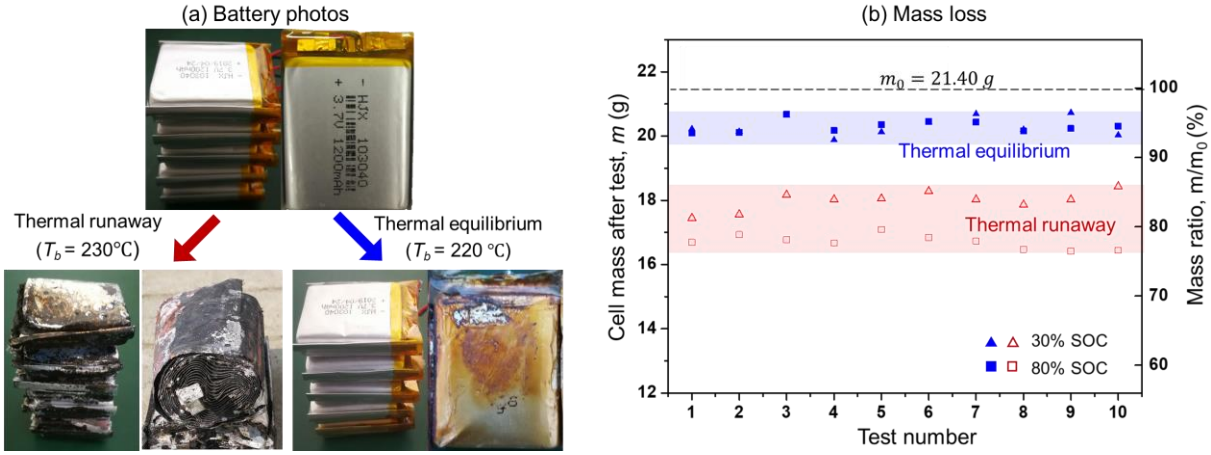

Figure 5. (a) photos of the 5-layer battery pile of 80% SOC before and after the experiment in Fig. 4, and (b) mass loss and the mass-loss ratio of battery cells after thermal runaway and thermal equilibrium.

Figure 5(a) further compares the photographs of the 5-layer battery pile before and after the experiment in Fig. 4. After the thermal runaway, all pouch cells are covered by black degraded electrolyte, and there were many small holes on the cell surface, which could be marks of bubbling and gas release from internal reactions. As shown in Fig. 5(b), about 20% of the original mass (i.e., about 4.5 g) is lost via the form of smoke. Also, a higher SOC of 80% leads to a 5% (or 1 g) more mass loss, agreeing with more smoke release observed in the experiment.

If reaching the thermal equilibrium (Fig. 5a), only the lower surface of the bottom cell become scorched brown with a limited electrolyte adhering to surface. At the same time, all other cells only show a small degree of swelling, compared to the untested cells. Compared to the case of thermal runaway, the mass loss is much smaller (Fig. 5b). That is, only about 5% of the original mass (or 1 g) is lost, because the smoke release is much smaller, as compared in Fig. 4. Moreover, the mass loss of these non-ignited cells is not sensitive to SOC.

3.2. Temperature and voltage evolution

Figure 6 shows the typical temperature and voltage evolution curves during the self-heating process for 80%-SOC battery cell: (a,b) single cell with well-insulated condition, and (c,d) 3 cells under the good top cooling condition. For the case of thermal runaway (Fig. 6a,c), there are three clear stages, (I) heating up, (II) self-heating to thermal runaway, and (III) cooling.

The swelling of battery occurs in the Stage (I), which indicates the start of some weak decomposition reactions. In Stage (II), the effect of self-heating becomes clear. The temperature of the battery cell exceeds the hot-boundary temperature, so that the hot-plate starts to cool the bottom battery cell. However, the cooling from the hot plate is not sufficient, as the temperature increasing rate reaches 0.05 °C/s and continues to accelerate, where more exothermic reactions inside the battery are initiated.

Then, the battery exceeds 500 °C in a short period time, where the heating rate of battery exceeds 15 °C/s, and a large amount of smoke are produced (i.e., the thermal runaway or successful self-ignition). Afterwards, in Stage III, the battery cell slowly cools down to below the hot plate temperature.

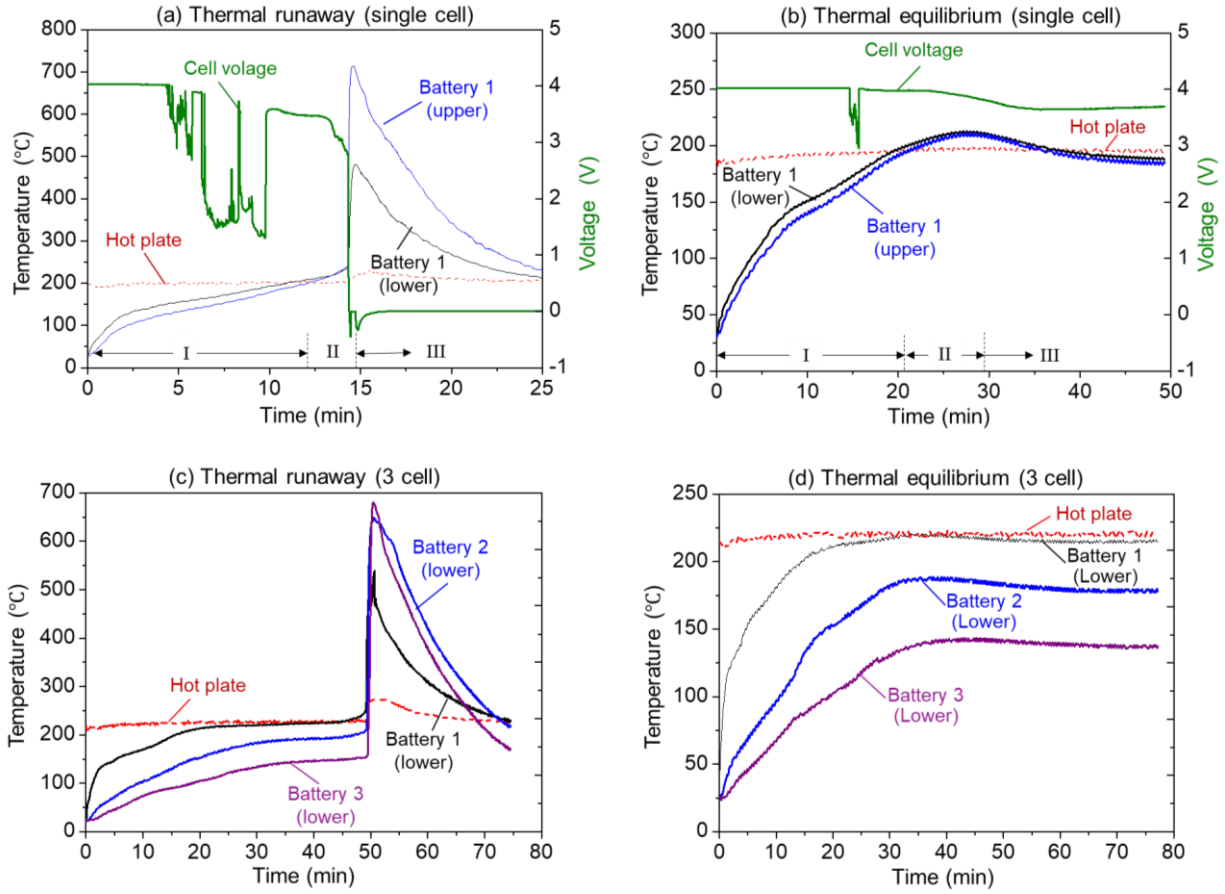

Figure 6. The temperature and voltage evolution for 80% SOC battery: (a) thermal runaway for single cell with well-insulated condition at the hot plate of 201 °C; (b) thermal equilibrium for a single cell with well-insulated condition at the hot plate of 196 °C, (c) thermal runaway for a 3-cell battery pile under a good top cooling condition at the hot plate of 225 °C; and (b) thermal equilibrium for a 3-cell battery pile under a good top cooling condition at the hot plate of 220 °C.

The battery will misfunction at a high temperature, indicated by the loss of voltage. Generally speaking, the voltage of Li-ion batteries is related to the materials inside the batteries [27]. When the internal short circuit occurs, the electrochemical energy stored in the materials inside the batteries will release [28]. When the temperature of the battery excesses a certain temperature, some components inside the battery start to decompose, which causes the voltage fluctuates. Figure 6(a) shows that the voltage of the battery keeps stable at the initial heating stage. When the temperature of the battery exceeded about 165 °C, its voltage shows a rapid drop, indicating the *potential failure of battery*. Then, the voltage starts fluctuating and never turns back to the original value. At the moment of thermal runaway, the voltage suddenly dropped to 0 V or some negative value, indicating that the battery is completely destroyed.

For the case of thermal equilibrium (Fig. 6b,d), there are also three stages. In Stage II, despite that the battery temperature clearly exceeds the hot plate up to about 20 °C, its maximum heating rate is lower than 0.05 °C/s and continuously decreases. Therefore, the bottom boundary successfully cools down the battery and prevent triggering additional exothermic reactions inside the battery. Afterwards, the battery slowly cools down to below the hot plate temperature and reaching the thermal equilibrium.

Therefore, the temperature evolution is found to be the same as conventional self-heating ignition process of organic solid fuels [21,29]. On the other hand, the battery voltage also shows a sudden drop near 165 °C, but it returns to the original voltage after a few minutes, and then slowly decreases to a stable value of about 3.7 V. In other words, the battery is not fully failed, despite that it has some irrecoverable internal damage and a higher probability of failure in future operation.

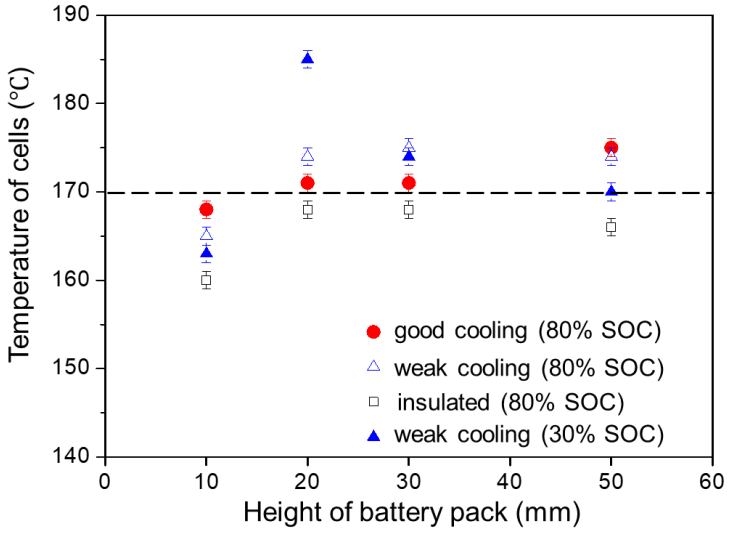

Figure 7. The potential failure temperature when the battery voltage begins to drop in different tests.

The potential failure temperature when the battery voltage begins to drop in different tests are summarized in Fig. 7. This failure temperature is almost constant, i.e., around 170 ± 5 °C, which is insensitive to the SOC, number of cells and environmental cooling condition. The drop of voltage could be a result of the melting of separator and the internal short circuit. Therefore, 170 °C could be close to the melting point of the battery separator, which is close to that in [30] while higher than 130 °C for prismatic battery with $LiCoO_2$ cathode [23].

3.3. Critical boundary temperature for thermal runaway

The major purpose of this experiment is to determine the critical hot boundary to trigger the thermal runaway of the battery pile (or the self-ignition temperature, T_b^*). Figure 8(a) summarizes how the critical boundary temperature varies with the height of battery piles. For the battery pile (a) with a good cooling condition, the critical thermal runaway temperature is almost stable and remains at 223 ± 2 °C. For the battery pile (b) with a poor cooling condition, the critical temperature of thermal runaway is much lower than that of (a). Moreover, this critical temperature increases slightly as the number of cells (N) or the height of the battery pile (H) increases. Specifically, the critical temperature of a single pouch cell is the lowest (208 °C), while for the 5-layer battery pile with a height of 50 mm, the critical temperature is 15 °C higher.

For the well-insulated battery pile (c), the critical boundary temperature of thermal runaway (T_b^*) further decreases to below 200 °C (the single cell case). Also, this critical temperature shows an increasing trend with the height, similar to case (b), while the maximum temperature increment is less than 10 °C. As the top environmental cooling condition ranks as (a) > (b) > (c), the critical temperature (T_b^*) ranks as (a) > (b) > (c). Therefore, we can conclude that a better cooling boundary condition leads to a higher critical boundary temperature for thermal runaway.

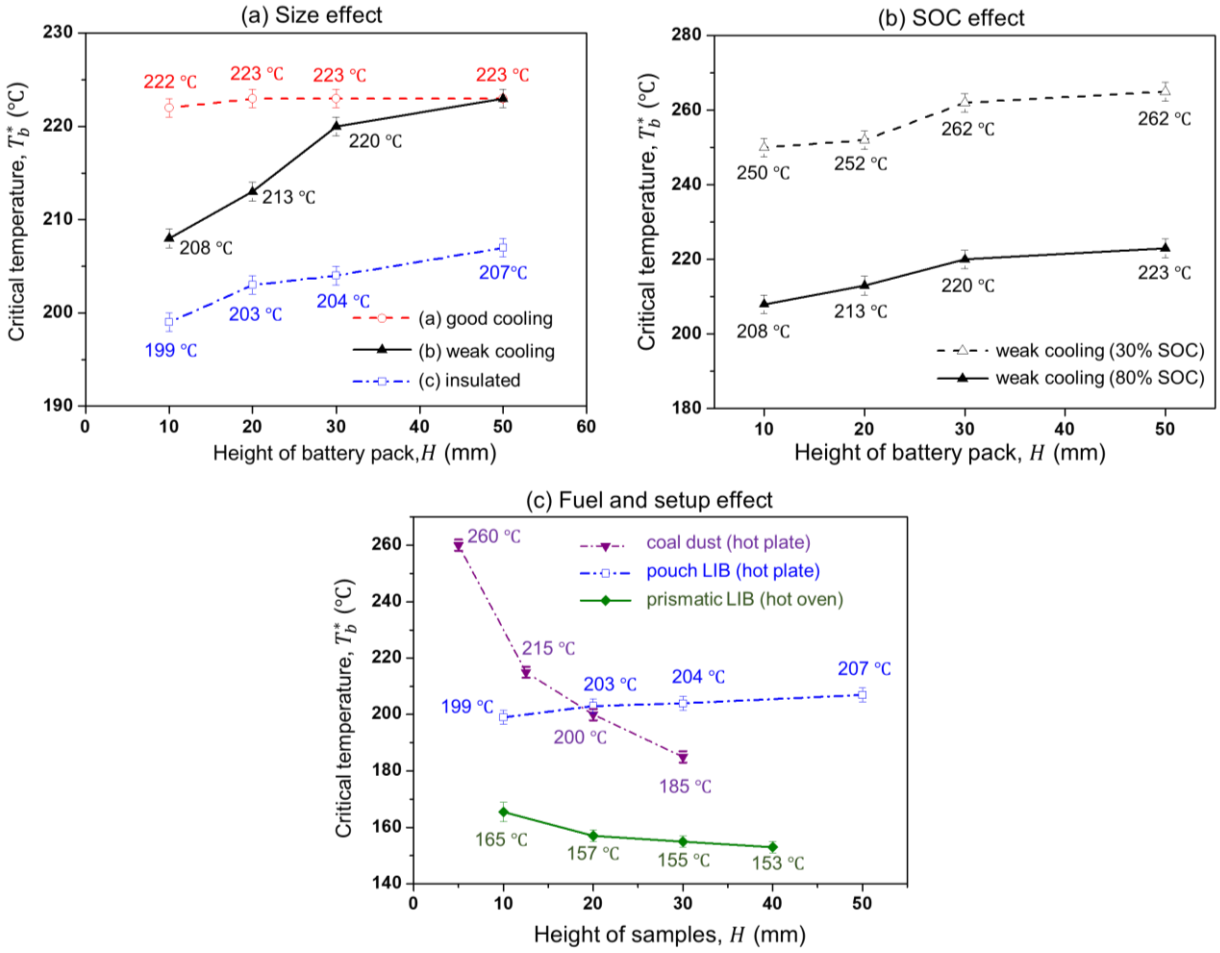

Figure 8. The critical self-ignition temperature (T_b^*) of battery pile: (a) 80% SOC under different top boundary cooling condition, (b) different SOCs under the weak cooling condition, and (c) compared to hot-plate test of coal dust [31] and the hot-oven test of prismatic battery cells [23].

Figure 8(b) quantifies the influence of SOC on the propensity of thermal runaway under a weak top boundary cooling condition of the battery pile. The critical temperature of both SOCs shows the same trend of increasing with the height of the battery pile. As expected, the critical self-ignition temperature at 30% SOC is about 40 °C higher than at 80% SOC. Therefore, the higher SOC means the higher self-heating ignition risk for the battery pile.

The trend of critical temperature slightly increasing with the thickness of the battery pile is opposite to other self-ignition tests of conventional hydrocarbon fuels [21,31,32]. Generally, the larger thickness of fuel results in better thermal insulation and limits the environmental cooling, so a lower bottom boundary temperature is needed to trigger the self-ignition [33]. For example, the critical self-ignition boundary temperature for a 5-mm thick coal dust layer is 260 °C, while reducing to 185 °C if the thickness increases to 30 mm [31], as compared in Fig. 8(c). Nevertheless, it has been found that in the hot-oven self-ignition test of prismatic Li-ion cells (up to 4 cells) [23], the critical ambient temperature decreases as the number of cells increases, which shows the same trend as hydrocarbon fuels, as compared in Fig. 8(c). Therefore, more experiments and analysis are required to conclude whether the self-ignition of battery is similar to conventional hydrocarbon fuels or not.

4. Discussions

4.1. Estimation of thermal conductivity

The effective thermal conductivity (k_e) plays an important role in the temperature distribution in the battery pile and the self-ignition risk. Once the battery pile reaches the thermal equilibrium (Fig. 9), the heat transfer through the battery pile is essentially a 1-D heat conduction process in the vertical direction.

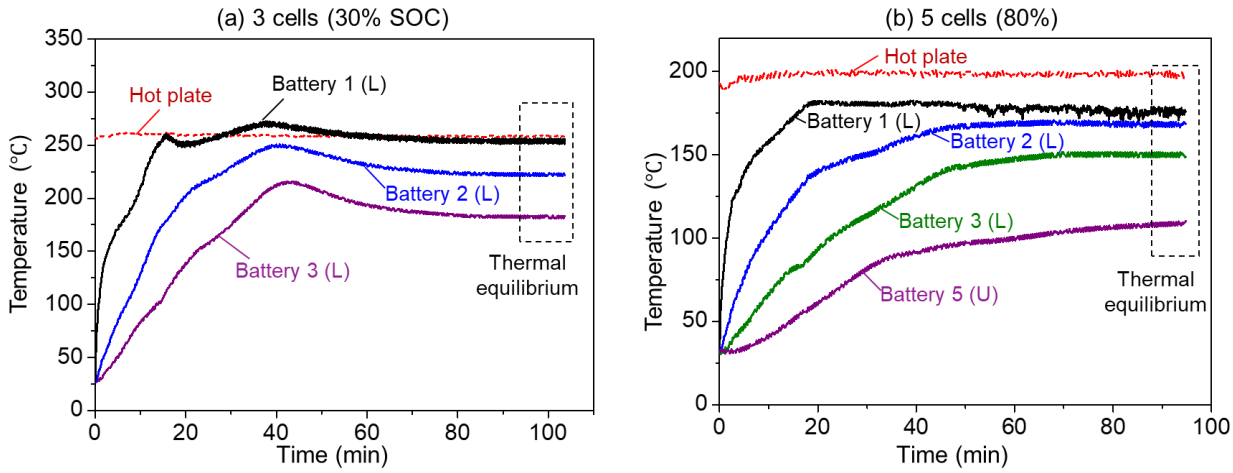

Figure 9. temperature curves approaching the thermal equilibrium at the subcritical condition with a good environmental cooling, (a) 3 cells (30% SOC) at the hot plate of 260 °C, and (b) 5 cells (80% SOC) at the hot plate of 200 °C, where L and U mean lower surface and upper surface, respectively.

As four sides of battery pile are surrounded by insulation board to limit the heat transfer in the horizontal direction, the 1-D heat transfer is a reasonable simplification (Fig. 10a). The bottom surface is under the constant temperature boundary condition. The major heat loss is the radiation and convection from the top surface to the environment, as

$$\dot{q}''_{loss} = h_c(T_s - T_a) + \varepsilon\sigma(T_s^4 - T_a^4) = h(T_s - T_a) \quad (1)$$

$$h = h_c + \varepsilon\sigma(T_s^2 + T_a^2)(T_s + T_a) \quad (2)$$

where T_b, T_s and T_a are the temperatures of the hot boundary, top surface of the battery pile, and ambient, respectively; ε is top surface emissivity which is 0.9 for the aluminum plastic film; and $\sigma = 5.67\times10^{-8}$ W/m^{2}K^4 is the Stefan–Boltzmann constant; h is overall cooling coefficient. The convective coefficient (h_c) can be expressed as:

$$h_c = C(T_s - T_a)^{\frac{1}{3}} \quad (3)$$

where C is an empirical coefficient for natural convection (1.52 for a horizontal plate) [34].

The thermal runaway had not happened yet, and the heat generation inside the battery is ignored. When the battery pile reaches the steady-state, heat flux through the battery equals the heat loss flux as

$$\dot{q}''_b = k_e \frac{T_b - T_s}{N\delta} = \dot{q}''_{loss} \quad (4)$$

where k_e is the effective thermal conductivity in the vertical direction of the battery, which also includes the effect of contact thermal resistant; ε is the emissivity; N is the layer number of battery pile; and δ = 10 mm is the thickness of one battery cell, respectively.

Based on Eqs. (1-4), k_e can be expressed as:

$$k_e = \frac{C(T_s - T_a)^{\frac{4}{3}} + \varepsilon\sigma(T_s^4 - T_a^4)}{T_b - T_s} N\delta \tag{5}$$

Table 2 lists some typical equilibrium temperature, calculated global environmental cooling coefficient, and the overall thermal conductivity of the pouch battery pile of different thicknesses, as well as their equivalent thermal resistant (R). Clearly, the value of k_e tends to decrease slightly, as the thickness of battery pile increases, mainly because more contact surface leads to a larger contact thermal resistant. For the first approximation, the effective thermal conductivity of the battery pile in the vertical direction is 0.30 ± 0.05 W/m-K.

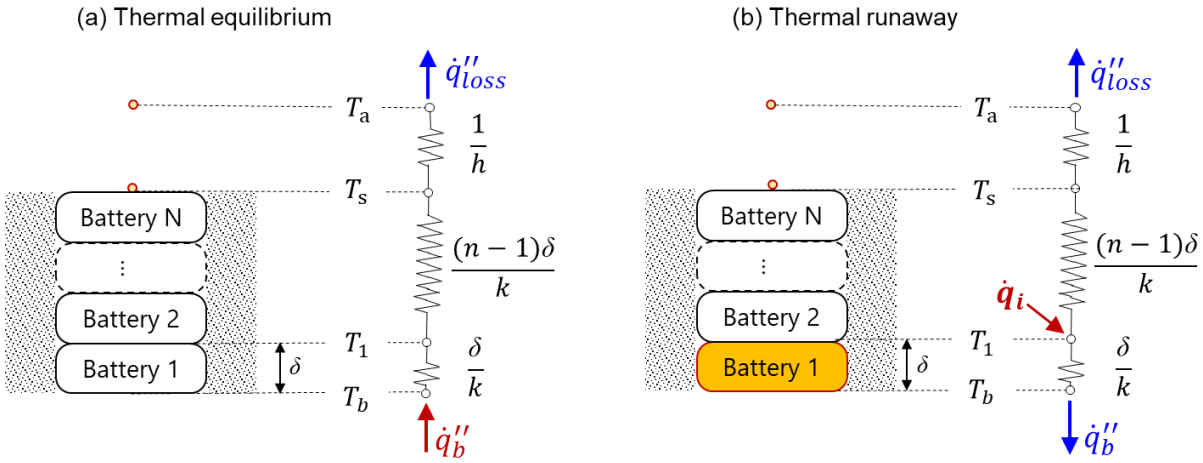

Figure 10. the schematic diagram of heat transfer: (a) thermal equilibrium, and (b) thermal runaway.

Note that the thermal resistance of this 10-mm thick pouch battery cell is only 33×10^{-3} m^{2}K/W. As compared in Table 2, this value is not only much smaller than the thermal resistance of coal dust (100×10^{-3} m^{2}K/W) and insulation board (83×10^{-3} m^{2}K/W), but it is also smaller than the thermal resistance of environmental cooling (about 67×10^{-3} m^{2}K/W). In other words, when the bottom battery cell (i.e., the most dangerous cell) gets hotter than the hot plate, having one battery cell above could cool the top surface (T_1 in Fig. 10) better than when it is directly cooled by the air.

Table 2. The equilibrium temperatures, effective thermal conductivity of battery (k_e) and the convective coefficient under a good top cooling condition (h), and corresponding thermal resistance (R).

N (-)	T_b (K)	T_s (K)	T_a (K)	nL (m)	$\dot{q}''$ (W/m^2)	h (W/m^{2}K)	$R_h = 1/h$ (m^{2}K/W)	k_e (W/mK)	$Bi=N\delta h/k_e$ (-)	$R_k = (N-1)\delta/k_e$ (m^{2}K/W)
1	218	157	23	0.01	2379	17.9	56×10^{-3}	0.39 ± 0.03	0.46	-
2	218	120	24	0.02	1470	15.5	65×10^{-3}	0.30 ± 0.02	1.03	33×10^{-3}
3	220	104	24	0.03	1160	14.5	69×10^{-3}	0.30 ± 0.02	1.45	67×10^{-3}
5	216	82	26	0.05	697	13.0	77×10^{-3}	0.26 ± 0.02	2.50	154×10^{-3}
10 mm coal dust, $R_k = \delta/k_e$								0.10		100×10^{-3}
10 mm insulation, $R_k = \delta/k_e$								0.12		83×10^{-3}

4.2. *Simplified heat analysis for environmental cooling effect*

Considering the case of a thermal runaway at the supercritical condition, when the temperature of the bottom battery cell exceeds the hot plate, the hot plate starts to cool the cell at the rate of $\dot{q}_b''$, as illustrated in Fig. 10b. For simplicity, a heat release rate ($\dot{q}_i$) of the bottom battery is assumed to balance the upward ($\dot{q}_{loss}''$) and downward heat dissipation ($\dot{q}_b''$). The heat balance equation can be expressed as:

$$\dot{q}_i = \dot{q}_i''' V = A(\dot{q}_b'' + \dot{q}_{loss}'') \tag{6}$$

where V is the volume of the battery cell; A is the contact area of the upper and lower surfaces of the battery. The heat release rate is controlled by the exothermic chemical reaction of the battery, which may be represented by a 1-step Arrhenius equation as

$$\dot{q}_i''' = Z \exp\left(-\frac{E}{RT_{LIB}}\right)\Delta H \tag{7}$$

where Z is the pre-exponential factor; E is activation energy; T_{LIB} is the temperature of the bottom Li-ion battery cell; and ΔH is heat of reactions, respectively. Then, Eq. (5) can be expressed as

$$Z\,exp\left(-\frac{E}{RT_1}\right)\Delta H\,\left(\frac{V}{A}\right) = k_e\frac{T_{LIB}-T_b}{\delta} + \frac{T_{LIB}-T_a}{1/h+(n-1)\delta/k_e} \tag{8}$$

If the characteristic temperature of the thermal runaway of the battery is assumed to be constant as T_{LIB}^*, the critical boundary temperature (T_b^*) can be expressed as

$$T_b^* = \frac{T_{LIB}^* - T_a}{k_e/h\delta + (n-1)} + C \tag{9}$$

$$C = T_{LIB}^* - Z\exp\left(-\frac{E}{RT_{LIB}^*}\right)\Delta H\,\left(\frac{V}{A}\right)\left(\frac{\delta}{k_e}\right) \tag{10}$$

where C is a constant. Therefore, Eq. (8) first demonstrates that the critical hot boundary temperature (T_b^*) increases with the heat transfer coefficient (h) at the top surface. This agrees with the experimental data in Fig. 8(a) where a higher boundary temperature for a better environmental cooling condition. In addition, the heat of reactions ΔH is roughly proportional to SOC for a variety of lithium ion chemistries [35], indicating that the critical hot boundary temperature (T_b^*) decreases with the SOC, which is consistent with experimental data in Fig. 8(b) where the higher SOC means the higher self-heating ignition risk for the battery pile.

4.3. *Applicability of conventional self-ignition theory*

As shown in Fig. 8, the critical boundary temperature for battery self-ignition slightly increases with the thickness of the battery pile, the trend of which is opposite to other hydrocarbon fuels like coal dust. Moreover, in current experiments, the thermal runaway always occurs to the bottom battery cell that is next to the hot plate. However, for conventional hydrocarbon dust fuels, the location of initial thermal runaway (or the hottest spot) is not at the bottom fuel layer next to the hot plate, but at a distance above the hot plate [29,31]. There are some possible reasons:

1) *Discrete nature of battery cells.* Compared to the dust fuels which have smaller particle size and uniform properties, the uniformity of the battery pile is limited to the thickness of each battery cell. The thermal conductivity inside the cell is much larger than the effective thermal conductivity between cells. Therefore, the temperature profile within the battery pile is discontinuous, different

from dust fuels.

2) *Swelling effect*. As the battery temperature rises, gas is continuously generated within the cell, so that the battery cell will swell. Both the gas generation and volume expansion reduce heat dissipation between cells. On the other hand, depending on the packing condition (e.g. loosely or tightly packed), the swelling of cells can either improve or diminish the contact condition between cells, which plays an important role in the heat dissipation between cells [36].

3) *Chemical effect*. For the exothermic reactions inside the battery, it does not need oxygen from the atmosphere [12,13], which is different from the hydrocarbon fuels or combustion reactions. For the hydrocarbon fuel closer to the free surface, the oxygen supply is better, which also drives the oxidation front move towards the free surface [29,37]. This may also explain why the thermal runaway always first occurs to the bottom cell, despite of having the worst oxygen supply. Comparatively, the hottest location of hydrocarbon dust tends to be closer to the free surface.

It is worth further investigating the influence of battery cell size, swelling, and non-oxidative battery chemistry on the self-heating behaviors of battery and the applicability of the conventional self-ignition theory. Additional experiments and numerical simulations will also be needed for quantitative analysis.

5. Conclusions

It is a novel experiment to study the self-heating ignition behavior of open-circuit pouch Li-ion battery piles under a hot boundary condition which follows the classical hot-plate test. We found that the thermal runaway of battery due to self-heating occurs on the hot plate. The thermal runaway always first occurs to the cell next to the hot plate and then propagates to upper cells at an interval of about 20 s. Before the thermal runaway, the thickness of battery cell will expand 20%, and the battery voltage is found to have a sudden drop at 170 ± 5 °C, insensitive to SOC or packing and environmental conditions. The effective thermal conductivity of the battery is measured to be 0.30 ± 0.05 W/m-K.

The critical boundary temperature for thermal runaway (T_b^*) ranges from 199 °C to 262 °C. This critical temperature is increased by 20 °C under a good environmental cooling condition whereas it is reduced by 40 °C as the SOC increases from 30% to 80%. Moreover, the critical boundary temperature for self-heating ignition slightly increases with the height of the battery pile. This trend is opposite to both the hot-plate self-ignition test of conventional hydrocarbon fuels and the hot-oven test of the battery. In other words, the classic self-heating ignition theory may not be completely applicable to predict the critical condition for the thermal runaway of some Li-ion batteries. This research explores new self-ignition phenomena to help understand the safety of open-circuit Li-ion battery piles during storage and transport. More experiments and numerical simulations are needed to reveal more insights into these special behaviors in future work.

Acknowledgements

The authors (PS and XH) would like to thank the support from HK Research Grant Council through the Early Career Scheme (25205519), Shanghai Science and Technology Committee (19160760700), and HK PolyU (G-YBZ1). HN is supported by the Guangdong Technology Fund (2015B010118001) and National Key R&D Program of China (2018YFB0104100). Authors thanks Xuanze He (Imperial College London) for valuable comments.

References

[1] G. Crabtree, Perspective: The energy-storage revolution, Nature. 526 (2015) S92–S92. doi:10.1038/526S92a.

[2] E.C. Evarts, Lithium batteries: To the limits of lithium, Nature. 526 (2015) S93–S95. doi:10.1038/526S93a.

[3] H.J. Noh, S. Youn, C.S. Yoon, Y.K. Sun, Comparison of the structural and electrochemical properties of layered Li[NixCoyMnz]O2 (x = 1/3, 0.5, 0.6, 0.7, 0.8 and 0.85) cathode material for lithium-ion batteries, J Power Sources. 233 (2013) 121–130. doi:10.1016/j.jpowsour.2013.01.063.

[4] U. Irfan, Battery Fires Reveal Risks of Storing Large Amounts of Energy, Sci Am. (2011).

[5] P. Sun, H. Niu, X. Huang, A Review of Fire in Electric Vehicles Powered by Lithium-ion Battery, Fire Technol [Accepted]. (2019).

[6] BBC News, Samsung Note 7 bombing investigation results: battery design problems, (2017).

[7] BBC News, Tesla Model S battery caught on fire 'without accident', says owner – Tesla is investigating, (2018).

[8] Yahoo News, Tesla car catches fire in Hong Kong parking lot: media, (2019).

[9] CNN Business, Tesla is updating its battery software after a car caught fire, (2019).

[10] P.G. Balakrishnan, R. Ramesh, T. Prem Kumar, Safety mechanisms in lithium-ion batteries, J Power Sources. 155 (2006) 401–414. doi:10.1016/j.jpowsour.2005.12.002.

[11] F. Larsson, B.-E. Mellander, Abuse by External Heating, Overcharge and Short Circuiting of Commercial Lithium-Ion Battery Cells, J Electrochem Soc. 161 (2014) A1611–A1617. doi:10.1149/2.0311410jes.

[12] Q. Wang, P. Ping, X. Zhao, G. Chu, J. Sun, C. Chen, Thermal runaway caused fire and explosion of lithium ion battery, J Power Sources. 208 (2012) 210–224. doi:10.1016/j.jpowsour.2012.02.038.

[13] Q. Wang, B. Mao, S.I. Stoliarov, J. Sun, A review of lithium ion battery failure mechanisms and fire prevention strategies, Prog Energy Combust Sci. 73 (2019) 95–131. doi:10.1016/j.pecs.2019.03.002.

[14] P. Ribière, S. Grugeon, M. Morcrette, S. Boyanov, S.S. Laruelle, G. Marlair, P. Ribiere, S. Grugeon, M. Morcrette, S. Boyanov, S.S. Laruelle, G. Marlair, P. Ribi, S. Grugeon, M. Morcrette, S. Boyanov, B. St Ephane Laruelle, G. Marlair, Investigation on the fire-induced hazards of Li-ion battery cells by fire calorimetry, Energy Environ Sci. 5 (2012) 5271–5280. doi:10.1039/C1EE02218K.

[15] X. Liu, S.I. Stoliarov, M. Denlinger, A. Masias, K. Snyder, Comprehensive calorimetry of the thermally-induced failure of a lithium ion battery, J Power Sources. 280 (2015) 516–525. doi:10.1016/j.jpowsour.2015.01.125.

[16] X. Liu, Z. Wu, S.I. Stoliarov, M. Denlinger, A. Masias, K. Snyder, Heat release during thermally-induced failure of a lithium ion battery: Impact of cathode composition, Fire Saf J. 85 (2016) 10–22. doi:10.1016/j.firesaf.2016.08.001.

[17] D. Finegan, M. Scheel, J.B. Robinson, B. Tjaden, I. Hunt, T.J. Mason, J. Millichamp, M. Di Michiel, G.J. Offer, G. Hinds, D.J.L. Brett, P.R. Shearing, In-operando high-speed tomography of lithium-ion batteries during thermal runaway., Nat Commun. 6 (2015) 6924. doi:10.1038/ncomms7924.

[18] A. Abaza, S. Ferrari, H.K. Wong, C. Lyness, A. Moore, J. Weaving, M. Blanco-Martin, R. Dashwood, R. Bhagat, Experimental study of internal and external short circuits of commercial automotive pouch lithium-ion cells, J Energy Storage. 16 (2018) 211–217. doi:10.1016/j.est.2018.01.015.

[19] X. Zhu, Z. Wang, Y. Wang, H. Wang, C. Wang, L. Tong, M. Yi, Overcharge investigation of large format lithium-ion pouch cells with Li(Ni 0.6 Co 0.2 Mn 0.2)O 2 cathode for electric vehicles:

Thermal runaway features and safety management method, Energy. 169 (2019) 868–880. doi:10.1016/j.energy.2018.12.041.

[20] S. Gao, X. Feng, L. Lu, N. Kamyab, J. Du, P. Coman, R.E. White, M. Ouyang, An experimental and analytical study of thermal runaway propagation in a large format lithium ion battery module with NCM pouch-cells in parallel, Int J Heat Mass Transf. 135 (2019) 93–103. doi:10.1016/j.ijheatmasstransfer.2019.01.125.

[21] V. Babrauskas, Ignition Handbook, Fire Science Publishers/Society of Fire Protection Engineers, Issaquah, WA, 2003. doi:10.1023/B:FIRE.0000026981.83829.a5.

[22] C. Toczauer, Cargo pallet catches fire at HKG, cause uncertain, Air Cargo World. (2019).

[23] X. He, F. Restuccia, Y. Zhang, Z. Hu, X. Huang, J. Fang, Experimental study of self-heating ignition of lithium-ion batteries during storage and transport : effect of the number of cells, Fire Technol (under Rev. (2019).

[24] J.T. Warner, The Handbook of Lithium-Ion Battery Pack Design: Chemistry, Components, Types and Terminology, Elsevier Science, 2015.

[25] S.T. Method, The Standard Test Method for Hot Surface Ignition Temperature of Dust Layers, ASTM D 2021-06, Am Soc Test Mater Int West Conshohocken. (2016) 1–10. doi:10.1520/E2021-15.2.

[26] S.T. Method, Standard Test Method for Hot-Surface Ignition Temperature of Dust Layers 1, (2019) 1–10. doi:10.1520/E2021-15.2.

[27] T. Utsunomiya, O. Hatozaki, N. Yoshimoto, M. Egashira, M. Morita, Self-discharge behavior and its temperature dependence of carbon electrodes in lithium-ion batteries, J Power Sources. (2011). doi:10.1016/j.jpowsour.2011.05.066.

[28] X. Feng, M. Ouyang, X. Liu, L. Lu, Y. Xia, X. He, Thermal runaway mechanism of lithium ion battery for electric vehicles: A review, Energy Storage Mater. 10 (2018) 246–267. doi:10.1016/j.ensm.2017.05.013.

[29] H. Yuan, F. Restuccia, F. Richter, G. Rein, A computational model to simulate self-heating ignition across scales, configurations, and coal origins, Fuel. 236 (2019) 1100–1109. doi:10.1016/j.fuel.2018.09.065.

[30] C.J. Orendorff, The role of separators in lithium-ion cell safety, Electrochem Soc Interface. (2012). doi:10.1149/2.F07122if.

[31] D. Wu, X. Huang, F. Norman, F. Verplaetsen, J. Berghmans, E. Van den Bulck, Experimental investigation on the self-ignition behaviour of coal dust accumulations in oxy-fuel combustion system, Fuel. 160 (2015) 245–254. doi:10.1016/j.fuel.2015.07.050.

[32] F. Restuccia, X. Huang, G. Rein, Self-ignition of natural fuels: Can wildfires of carbon-rich soil start by self-heating?, Fire Saf J. 91 (2017) 828–834. doi:10.1016/j.firesaf.2017.03.052.

[33] J. Garcia Torrent, N. Fernandez Anez, L. Medic Pejic, L. Montenegro Mateos, Assessment of self-ignition risks of solid biofuels by thermal analysis, Fuel. (2015). doi:10.1016/j.fuel.2014.11.074.

[34] F.P. Incropera, Fundamentals of heat and mass transfer, John Wiley, 2007.

[35] R.E. Lyon, R.N. Walters, Energetics of lithium ion battery failure, J Hazard Mater. 318 (2016) 164–172. doi:10.1016/j.jhazmat.2016.06.047.

[36] M. Hao, J. Li, S. Park, S. Moura, C. Dames, Efficient thermal management of Li-ion batteries with a passive interfacial thermal regulator based on a shape memory alloy, Nat Energy. 3 (2018) 899–906. doi:10.1038/s41560-018-0243-8.

[37] X. Huang, G. Rein, Upward-and-downward spread of smoldering peat fire, Proc Combust Inst. 37 (2019) 4025–4033. doi:10.1016/j.proci.2018.05.125.